Biochimie 93 (2011) 730–741

Contents lists available at ScienceDirect

Biochimie

journal homepage: www.elsevier.com/locate/biochi

Research paper

Mutation in the substrate-binding site of aminopeptidase B confers new enzymatic properties

Viet-Laï Pham [a], Cécile Gouzy-Darmon [a], Julien Pernier [a], Chantal Hanquez [a], Vivian Hook [b], Margery C. Beinfeld [c], Pierre Nicolas [a], Catherine Etchebest [d], Thierry Foulon [a], Sandrine Cadel [a,*]

[a] UPMC Univ Paris 06, ER3 BIOSIPE, BIOgenèse des SIgnaux PEptidiques, F-75005, Paris, France
[b] Skaggs School of Pharmacy and Pharmaceutical Sciences, University of California, San Diego, La Jolla, California, USA
[c] Department of Pharmacology and Experimental Therapeutics, Tufts University, School of Medicine, Boston, MA 02111, USA
[d] Université Paris Diderot-Paris7, Equipe Dynamique des Structures et des Interactions des Macromolécules Biologiques UMR S 665, INSERM, INTS Paris F-75739, France

ARTICLE INFO

Article history:
Received 3 November 2010
Accepted 24 December 2010
Available online 13 January 2011

Keywords:
Zn^{2+}-metallopeptidase
Miniglucagon
Hormone processing
Neuropeptide processing
Leukotriene A_4 hydrolase
M1 family

ABSTRACT

Aminopeptidase B (Ap-B) catalyzes the cleavage of arginine and lysine residues at the N-terminus of various peptide substrates. *In vivo*, it participates notably in the miniglucagon and cholecystokinin 8 processing, but the complete range of physiological functions of Ap-B remains to be discovered. Ap-B is a member of the M1 family of Zn^{2+}-metallopeptidases that are characterized by two highly conserved motives, GXMEN (potential substrate binding site) and HEXXHX^{18}E (Zn^{2+}-binding site). In this study, mutagenesis and molecular modelling were used to investigate the enzymatic mechanism of Ap-B. Nineteen rat Ap-B mutants of the $G_{298}XM_{300}E_{301}N_{302}$ motif and one mutant of the $HEIS_{328}HX^{18}E$ motif were expressed in *Escherichia coli*. All mutations except $G_{298}P$, $G_{298}S$, and $S_{328}A$ abolished the aminopeptidase activity. The $S_{328}A$ mutant mimics the sequence of bovine Ap-B Zn^{2+}-binding site, which differs from those of other mammalian Ap-B. This mutant conserved a canonical Ap-B activity. $G_{298}S$ and $G_{298}P$ mutants exhibit new enzymatic properties such as changes in their profile of inhibition and their sensitivity to Cl^- anions. Moreover, the $G_{298}P$ mutant exhibits new substrate specificity. A structural analysis using circular dichroism, fluorescence spectroscopy, molecular modelling and dynamics was performed to investigate the role that residue G_{298} plays in the catalytic mechanism of Ap-B. Our results show that G_{298} is essential to Ap-B activity and participates to the substrate specificity of the enzyme.

1. Introduction

NRD convertase [1] and Cathepsin L [2] cleave prohormones on the NH_2-terminus side of basic amino acid doublets. Aminopeptidase B (Ap-B) hydrolyses Arg or Lys residue at the NH_2-terminus of various peptides [3]. Working together, these peptidases process somatostatin-28 into somatostatin-14 *in vitro* [4,5], glucagon into miniglucagon in the α-cells of the islets of Langerhans [6,7], enkephalins in various tissues [8], cholecystokinin in mouse brain [9] and POMC in the pituitary [10].

Ap-B is a secreted enzyme ubiquitously expressed in mammals and whose expression level is both tissue- and species-dependent [3,11–16]. *In vitro*, Ap-B has also a residual capacity to hydrolyze leukotriene A_4 (LTA_4) into the pro-inflammatory lipid mediator leukotriene B_4 (LTB_4) [12]. The bi-functional nature of Ap-B is supported by a close structural relationship with LTA_4 hydrolase (LTA_4H; EC 3.3.2.6; 33% identity, 48% similarity) [12], which hydrolyses LTA_4 into LTB_4 *in vivo*, and

Abbreviations: ACE, angiotensine converting enzyme; Ap-A, glutamyl aminopeptidase; Ap-B, aminopeptidase B; Ap-N, aminopeptidase N; Ap-O, aminopeptidase O; Ap-Q, aminopeptidase Q; Bac-rAp-B, recombinant His-tagged rat aminopeptidase B produced from baculovirus infected insect cells; CCK, cholecystokinin; ERAP1, endoplasmic reticulum aminopeptidase 1; ERAP2, endoplasmic reticulum aminopeptidase 2; His-rAp-B, recombinant His-tagged rat aminopeptidase B produced from *E. coli*; IRAP, insulin regulated membrane aminopeptidase; L-aa β-NA, L-amino acid β-naphthylamide; LTA_4, leukotriene A_4; LTB_4, leukotriene B_4; LTA_4H, leukotriene A_4 hydrolase; PSA, puromycin sensitive aminopeptidase; rAp-B, rat aminopeptidase B; tACE, testis angiotensine converting enzyme; TRH-DE, thyrotropin-releasing hormone degrading enzyme.

* Corresponding author at: ER3 UPMC, Biogenèse des signaux peptidiques, Université Pierre et Marie Curie, Bâtiment A, 5ème étage, Case courrier 29, 7 Quai Saint-Bernard, 75005 Paris, France. Tel.: +33 1 44272172; fax: +33 1 44273699.

E-mail addresses: vietlai_2000@yahoo.com (V.-L. Pham), cecile.darmon@upmc.fr (C. Gouzy-Darmon), julien.pernier@upmc.fr (J. Pernier), chantal.hanquez@upmc.fr (C. Hanquez), vhook@ucsd.edu (V. Hook), margery.beinfeld@tufts.edu (M.C. Beinfeld), pierre.nicolas@upmc.fr (P. Nicolas), catherine.etchebest@inserm.fr (C. Etchebest), thierry.foulon@upmc.fr (T. Foulon), marie-sandrine.cadel@upmc.fr (S. Cadel).

0300-9084/$ – see front matter © 2011 Elsevier Masson SAS. All rights reserved.
doi:10.1016/j.biochi.2010.12.015

exhibits an aminopeptidase activity *in vitro* [17]. Both enzymes belong to the M1 family of Zn^{2+}-dependent metallopeptidases whose members are characterized by the presence of two conserved motives in their primary structures, GXMEN and $HEXXHX^{18}E$ [12,15,17–21]. A 3D model of Ap-B was constructed [22] based on the crystal structure of human LTA_4H in complex with zinc ion and bestatin [23].

The catalytic mechanism of the enzymes belonging to the M1 family was originally deduced from that of thermolysine (M4 family of Zn^{2+}-endoproteases) [24] and was recently detailed for LTA_4H [25]. The $HEXXHX^{18}E$ motif is involved in the binding of the Zn^{2+} cation. In the absence of substrate, the zinc atom is tetracoordinated by the histidine residues, the second glutamate residue of this pattern, and a water molecule. Once the substrate is bound in the active site, it displaces the zinc-associated water molecule and chelates the zinc ion by its free amine and carbonyl oxygen [25]. The first glutamate of the pattern participates to the catalysis reaction, probably acting as a general base in the nucleophilic attack of the carbonyl group of the peptide bond, and as an acid catalyst to give a proton to the leaving amine moiety [25]. Although Ap-B and LTA_4H from Mammals show a highly conserved sequence of the Zn^{2+}-binding motif (HEISH), bovine Ap-B [26] exhibits a different sequence (HEIAH), which is found in several other aminopeptidases of the M1 family, e.g. the putative LTA_4H from *Drosophila melanogaster* (accession number Q7KT44), *Anopheles gambiae* (accession number Q7Q192), *Caenorhabditis elegans* (accession number O44183), and *C. briggsae* (accession number Q61MW9). Interestingly, bovine Ap-B shows a different substrate specificity compared to the rat enzyme, since it is able to preferentially cleave the Arg-methyl-coumarin (MCA) substrate, but also to a lesser extend: Asn-, Leu-, Met-, Asp-, Ser- and Lys-MCA substrates [26].

The GXMEN motif was proposed to participate to the transition state stabilization and to the aminopeptidase specificity. The glutamate and asparagine residues seem to be implicated in the binding of the NH_2-terminus of substrates [25,27–32]. Co-crystallisation of the LTA_4H-$E_{296}Q$ mutant with a tripeptide showed that hydrogen bonds are established between the carbonyl oxygen of the leaving P′1 residue of the substrate and the amide nitrogen of the glycine residue [25]. Analysis of mutations of this glycine residue in the GXMEN motif is difficult, since the function of this amino acid depends on the substrate specificity of the aminopeptidase and the rearrangement of the active site during the catalysis process.

Herein, 19 rat Ap-B (rAp-B) mutants of the $G_{298}XM_{300}E_{301}N_{302}$ motif were constructed and expressed in *Escherichia coli*. Among the 19 Ap-B mutants, only two mutations led to an active enzyme, $G_{298}P$ and $G_{298}S$. The $G_{298}S$ mutant conserves the Arg and Lys substrate specificity of the wild-type enzyme, whereas the $G_{298}P$ mutant gains a new activity against Ala and Pro residues at the N-terminus of L-amino acid β-naphthylamide (L-aa β-NA), together with a modified inhibition profile and a loss of Cl^- anion sensitivity. Analysis of the mutants using circular dichroism shows that $G_{298}P$ and $G_{298}S$ exhibit only small variations of secondary structures compared to rAp-B. Fluorescence spectroscopy on $G_{298}P$ and $G_{298}S$ mutants compare to the wild type protein does not reveal noteworthy variation. Molecular modelling and dynamics were also used to study these new enzymes and the role of the G_{298} residue in Ap-B.

Moreover, the $HEIA_{328}H$ mutant was constructed, expressed, purified to homogeneity, and characterized for its catalytic specificity, in order to analyze the effect of a bovine-like mutation in the HEISH motif of rAp-B. The results show that the $S_{328}A$ mutant and the recombinant rAp-B exhibit similar properties. This demonstrates that the alanine of this motif is not directly implicated in the substrate specificity of bovine Ap-B.

2. Materials and methods

2.1. Site-directed mutagenesis

The pIVEX2.4-Ap-B recombinant expression vector was used for site-directed mutagenesis [22] and mutants were generated with the QuickChange® Multi Site-Directed Mutagenesis kit according to the manufacturer specifications (Stratagene Europe, Amsterdam, Netherlands). This system allows randomizing (X) the targeted amino acid residues using oligonucleotides containing degenerate codons (site-specific saturation mutagenesis; see below). All the primers used for mutagenesis were 5′-phosphorylated. A single oligonucleotide per site was used in each experiment. The mutagenic codon was underlined in the oligonucleotide sequence. The targeted amino acids and their corresponding mutagenic primers were the followings: $G_{298}X$, 5′-CCATCTTTCCCGTTTNNNGGAATGGAGAATCCC-3′; $G_{298}S$, 5′-CCATCTTTCCCGTTTAGTGGAATGGAGAATCCC-3′; $G_{298}A$, 5′-CCATCTTTCCCGTTTGCGGGAATGGAGAATCCC-3′; $G_{298}P$, 5′-CCATCTTTCCCGTTTCCGGGAATGGAGAATCCC-3′; $M_{300}X$, 5′-CCCGTTTGGAGGANNNGAGAATCCCTGCCTG-3′; $E_{301}X$, 5′-CGTTTGGAGGAATGNNNAATCCCTGCCTGACC-3′; $N_{302}X$, 5′-TTTGGAGGAATGGAGNNNCCCTGCCTGACCTTT-3′; $S_{328}A$, 5′-TGTGCGCGATCTCGTGGATGATGACGTCGG-3′. Generated mutants were identified by direct sequencing on both strands using the dideoxy chain-termination procedure (Genome Express facilities, Meylan, France). The $G_{298}G$ conservative mutant presented in Table 1 constitute a positive control in the site-directed mutagenesis experiments. Other putative conservative mutants such as $M_{300}M$, $E_{301}E$ and $N_{302}N$ could also be considered as controls although their corresponding codon remains unchanged. However, it cannot be preclude that they come from the undigested pIVEX2.4-Ap-B parental DNA template. Some mutants, such as $G_{298}A/P/S$, were obtained by site-specific saturation mutagenesis and then by classical site-directed mutagenesis. The $S_{328}A$ mutant was constructed only by classical site-directed mutagenesis.

2.2. Production of rAp-B in E. coli

The pIVEX2.4-Ap-B recombinant plasmid was used to produce wild-type (His-rAp-B) and mutated recombinant rAp-B (NH_2-terminal His-tagged proteins) with a T7 promoter-driven system and a BLi5 *E. coli* strain as described in [22]. Briefly, 1 mL of LB medium supplemented with 20 μg/mL chloramphenicol and 100 μg/mL ampicillin were inoculated with Bli5 cells harbouring the pIVEX2.4-Ap-B plasmid and incubated overnight at 37 °C with agitation. The overnight culture was then diluted to 1:50 with 50 mL of fresh LB medium containing 100 μg/mL ampicillin and was grown under vigorous shaking at 37 °C until the OD_{600} reached 0.6. Isopropyl β-D-1-thiogalactoside (Sigma–Aldrich, Saint Quentin Fallavier, France) was added to a final concentration of 1 mM and the expression culture was grown at 37 °C under agitation for 2 hours. Cells were then harvested by centrifugation at 4000 × g for 5 min and stored at −80 °C until use or processed immediately as described below for western blotting, purification and enzymatic activity assays.

2.3. Production of rAp-B in baculovirus-infected cells

H5 cells were grown in liquid cultures (1 liter flask) at 28 °C in X-Press medium (BioWhittaker, France) supplied with fungizone (2.5 mg/mL; BioWhittaker, France) and gentamycine (50 mg/mL; BioWhittaker, France). Cells were infected at a density of 2×10^8 cells/liter with 1 mL of rAp-B-HIS-BAC virus stock expressing His-tagged rAp-B [33]. After 3 days of infection, cells were harvested by centrifugation 10 min at 1500 × *g* and the culture medium was collected. The recovered infected cell culture medium supernatant (500 mL) was concentrated to 200 mL and equilibrated

Table 1
Activity of wild type and mutated rat Ap-B.[a]

Mutation site	Number of mutants	Mutated codon	Mutants	Relative activity
G_{298}		**GGA**	**Wild type**	+++
	1	GGG	G	+++
	1	TTA	L	–
	2	GTA/GTT	V	–
	1	TTT	F	–
	1	ACA	T	–
	2	AGT	S	++
	2	GCG	A	–
	2	CCG	P	+++
M_{300}		**ATG**	**Wild type**	+++
	2	**ATG**	**M**	+++
	1	ACT	T	–
	1	AGA	R	–
	1	GAC	D	–
	1	CTG	L	–
E_{301}		**GAG**	**Wild type**	+++
	1	**GAG**	**E**	+++
	1	GGA	G	–
	1	GAC	D	–
	2	CCT	P	–
N_{302}		**AAT**	**Wild type**	+++
	1	**AAT**	**N**	+++
	3	CTC	L	–
	3	AAA	K	–
	1	TAT	Y	–
	1	TTT	F	–
S_{328}		**TCC**	**Wild type**	+++
	2	GCG	A	+++

[a] The number of mutants analyzed, the mutated codon and its corresponding amino acid, as well as the relative enzyme activity (+++, 80 to 100 % of activity; ++, 40 to 80 % of activity; –, no detected activity) are indicated. The position of the targeted amino acid in the rat Ap-B sequence is numbered. The relative enzyme activity was determined using L-Arg β-NA as substrate (see Materials and Methods section). These results are the average of three independent series of tests performed with all mutants (34 clones) in which each point was performed in triplicate.

in 20 mM Tris–HCl pH 8, using the Vivaflow 200 Tangential Flow Module (VivaSciences, France).

2.4. Purification of the recombinant His-rAp-B and mutants

pIVEX2.4-Ap-B transformed cell pellets from an expression culture (see above) were resuspended in 5 mL of lysis buffer (20 mM imidazole, 0.5 M NaCl, 20 mM Tris–HCl, pH 8) and sonicated, at 40 Mcycles, 5 times during 30 s at 4 °C. The extract was then centrifuged at 10,000 × *g* for 20 min at 4 °C to pellet the cellular debris. The supernatant was collected and mixed with Ni-NTA agarose (v/v; Qiagen, Hilden, Germany), which was pre-equilibrated with lysis buffer.

For the His-tagged rAp-B extracted from baculovirus infected cells (Bac-rAp-B), 5 mL of the recovered infected cell culture medium equilibrated in 20 mM Tris–HCl pH 8 were adjusted to 10 mL with 20 mM Tris–HCl pH 8 containing 20 mM imidazole and 0.5 M NaCl, and mixed with Ni-NTA agarose (v/v; Qiagen, Hilden, Germany).

The mixture was incubated with gentle mixing for 1 H at 4 °C and applied to a minicolumn for gravity flow chromatography. The column was washed 3 times with 3 to 5 mL of washing buffer (40 mM imidazole, 200 mM NaCl, 20 mM Tris–HCl, pH 8). Finally, the His-tagged purified protein was eluted by 4 to 6 successive elution steps with a buffer composed of 250 mM imidazole, 200 mM NaCl and 20 mM Tris–HCl at pH 8. Then, the purified protein was concentrated and equilibrated in 50 mM Tris–HCl pH 7.2 (or in 50 mM borate pH 7.4), 1 mM β-mercaptoethanol using a stirred ultrafiltration cell (Amicon, model 8050; Ultrafiltration membrane YM 30; Millipore Corporation, Bedford, MA, USA).

The determination of the protein concentrations in the different steps of the purification procedure was performed using the Bradford method. The concentration of the purified proteins was calculated using its molar absorbance coefficient (105,530 at 280 nm).

2.5. Western blotting

Western blotting was performed as described in [22]. Briefly, BLi5 or pIVEX2.4-Ap-B transformed cells (see above) were resuspended in PBS supplemented with 2 mg/mL lysozyme. Lysis was completed by 15 passages through a 25-gauge needle and 3 sonication steps of 1 min at 40 Mcycles at 4 °C. The protein extracts were centrifuged at 4000 × *g* during 5 min at 4 °C. The supernatants containing the soluble intracellular proteins were kept. Aliquots of protein extracts or purified proteins (see above) were run under denaturing conditions on an 8% polyacrylamide gel (SDS-PAGE). Then, they were transferred to a nitrocellulose membrane (0.45 μm, Schleicher and Schuell, Dassel, Germany) using a semi-dry blotting apparatus (Hoefer scientific instruments, San Francisco, USA). The rat Ap-B was detected with a specific anti-Ap-B polyclonal serum [3] at a dilution of 1:2000. Antigen-antibody complexes were visualized using a goat alkaline phosphatase coupled secondary antibody (Sigma–Aldrich, Saint Quentin Fallavier, France) and an NBT-BCIP mixture (Sigma–Aldrich, Saint Quentin Fallavier, France). SDS-PAGE gels were stained with silver salts to visualize total or purified proteins [22].

2.6. Enzyme activity assays

Ap-B activity was determined using L-aa β-NA substrates (Sigma–Aldrich; Saint Quentin Fallavier, France) and a specific inhibitor, arphamenine B (Sigma–Aldrich; Saint Quentin Fallavier, France) as previously described [22]. Briefly, protein extracts were pre-incubated with or without 1 μM arphamenine B for 15 min at 20 °C in assay buffer (50 mM Tris–HCl, pH 7.4) prior to incubation at 37 °C for 30 min in the assay buffer containing 0.2 mM L-aa β-NA. Hydrolysis was interrupted by the addition of 0.3 mL of freshly prepared colour reagent (Fast Garnet GBC salt; Sigma–Aldrich; Saint Quentin Fallavier, France). As a control, when crude extracts are used, assays were also performed in presence of 2 μM amastatine, a potent inhibitor of the aminopeptidase N of *E. coli*. This control allows, on one hand, to confirm the results obtained with arphamenine B, and on the other hand, to identify mutant proteins with certain changes in their inhibition profile, such as G_{298}P or G_{298}S. The absorbance was read at 535 nm using a spectrophotometer. The percentage of rAp-B activity, which is equivalent to the percentage of inhibition by arphamenine B, was measured by comparison with values obtained without inhibitor. In the case of G_{298}P and G_{298}S mutants, the percentage of rAp-B activity is equivalent to the percentage of activity retained after inhibition by amastatine.

To determine the effect of inhibitors on His-rAp-B, G_{298}S and G_{298}P activity, 1.5 μg of each purified proteins were preincubated in assay buffer in the presence of selected inhibitors for 10 min at 37 °C. Thirty minutes after the addition of the substrate, the reaction was stopped. The percentage of inhibition was measured by comparison with values obtained without inhibitor (Table 3).

2.7. Urea treatment

Purified His-rAp-B, Bac-rAp-B, G_{298}S and G_{298}P mutants were incubated in 50 mM Tris–HCl, pH 7.4 with various concentrations of urea (from 0 to 9 M) for 30 min at 20 °C before the remaining

activity of each sample was measured as described above. Assays were performed with and without 150 mM NaCl. The protein concentration was 30 nM for all experiments.

2.8. Effect of the temperature on Ap-B activity

Activities from purified His-rAp-B, Bac-rAp-B, $G_{298}S$ and $G_{298}P$ proteins (15 nM/assay) were measured after 10 min of pre-incubation at different temperatures (30, 37, 40, 45, 50, 55, 60, 65, 70, 75 and 80 °C) and an activity assay was performed as described in the section above. Activities are expressed relative to the maximum activity at 37 °C (100%) of each enzyme.

2.9. Circular dichroism and spectra analysis

Purified His-rAp-B, Bac-rAp-B, $G_{298}S$ and $G_{298}P$ proteins (5 μM in 50 mM borate, pH 7.4) were analyzed in a Jobin Yvon Dichrograph with a cell of 1 mm path length and a CD6 Dichrograph software (version 1.1, Instruments S.A./Jobin-Yvon). Spectral acquisition was carried out at 25 °C between 185 and 260 nm. Initial spectra represent four scans accumulated and averaged. Final spectra represent scans of several different samples accumulated and averaged (6 samples for His-rAp-B, 3 for Bac-rAp-B, 7 for $G_{298}P$, 5 for $G_{298}S$). All spectra were corrected by subtraction of the background obtained with protein-free samples at 25 °C. Calculation of different secondary structure contents was made using the Dichroprot V2.5 software (Institut de Biologie et Chimie des Protéines, CNRS-UPR412, Lyon, France).

2.10. Fluorescence spectroscopy

Fluorescence spectra of His-rAp-B, Bac-rAp-B, $G_{298}S$ and $G_{298}P$ were recorded at 25 °C with a PTI spectrometer (55–65 W; Photon Technology International, Birmingham, NJ, USA) in a 5 mm path-length quartz cell. The excitation wavelength was set at 280 nm, and the fluorescence emission spectra were scanned from 305 to 505 nm. The protein concentration was 1 μM for all experiments and all spectra were corrected for the buffer absorption.

2.11. Molecular modelling and mutant construction

The Ap-B homology model was constructed [22] with Modeller package 6.2 version using the 3D structure of the LTA_4H in complex with zinc ion and bestatin as a template (1hs6.pdb) [23]. In the model, we do not consider the bestatin molecule because further theoretical parameters are required for optimizing the whole complexed structure. Moreover, in the template structure, the bestatin molecule is located in a tunnel-like cavity and leaving the cavity free permits a comparison of the difference or similarities in the physico-chemical features of the tunnel in both structures [22]. The mutants $G_{298}S$ and $G_{298}P$ were constructed by substitution of the corresponding side-chain in the wild type structure. The percentage of sequence identity between LTA_4H and Ap-B in the region covering the motives GXMEN and $HEXXHX^{18}E$ (amino acids 290–350) is 78%. The side-chains conformation was then refined using Scwrl3.0 [34]. Zinc ion was placed in an equivalent position as observed in the crystal structure of LTA_4H (1HS6.pdb) [23].

2.12. Molecular dynamic protocol

The simulations were performed with the Gromacs package 3.3 [35–38] using Gromos96-53a6 force field [39] and SPC-type water molecules. We chose to protonate His residues 38, 325, 329 on Nδ1 atom, while others were protonated on Nε2 atom. The system was solvated in a water box and neutralized with 14 positive Na^+ ions. Depending on the mutant type, the system contained more than 22,200 water molecules. The system was initially minimized, then heated to 300 K. Three first runs were done with position restraints applied on protein heavy atoms and gradually relaxed. Electrostatic interactions were treated with a generalized reaction-field approach for distances larger than 18 Å where the dielectric value was 78. Van der Waals interactions were cut above 14 Å. The non-bonded list was updated every 10 steps. The simulations were carried out in NPT conditions, with Berendsen algorithm for coupling. The protein, solvent, and ions were separately coupled to the temperature bath. The pressure was fixed to 1 bar with a compressibility of 4.6×10^{-5} bar^{-1}. t_T and t_P coupling constants were respectively 0.1 and 0.5. All bonds were constrained with the Lincs algorithm and a 2 fs integration time-step was used. Simulations were carried for more than 5 ns. Gromacs tools were used for the analysis. The distances between center of masses of residues were computed with g_dist tool.

3. Results

3.1. Site-directed mutagenesis

Site-directed mutagenesis was performed on 5 residues (underlined) located in the conserved $\underline{G_{298}}X\underline{MEN}$ and Zn^{2+}-binding $HEX\underline{S}H$ motives (Table 1). Several mutants were obtained using one degenerate codon-containing oligonucleotide in order to generate mutant collections. All mutants were expressed in Bli5 *E. coli* strain and showed a single band on western blot, similar to wild type enzyme (data not shown). Activity assays in absence or in presence of arphamenine B, an Ap-B inhibitor, were performed with crude protein extracts (Table 1).

3.1.1. $S_{328}A$ mutation in the $HEIS_{328}HX^{18}E$ Zn^{2+}-binding motif

The sequence of the bovine Ap-B Zn^{2+}-binding motif is $HEIAHX^{18}E$ [26] whereas this sequence is $HEISHX^{18}E$ in all other Ap-Bs and LTA_4Hs from Mammals. Consequently, we constructed the corresponding His-rAp-B mutant to investigate potential differences in enzymatic activity and specificity. $S_{328}A$ mutants were expressed in Bli5 *E. coli* strain, and recombinant proteins were purified and checked by SDS-PAGE and western blot. Gel electrophoresis and western blotting of the purified His-rAp-B and $S_{328}A$ proteins show a single band with a relative molecular mass around 74 kDa (data not shown). These experiments also show that recombinant proteins are properly expressed in this prokaryotic expression system and that no degradation product was present in the purified enzymes.

Activity assays in absence or in presence of arphamenine B were performed in triplicate with the purified enzymes using L-aa β-NA representing the 20 amino acids. No modification of enzymatic activity or specificity was observed with the $S_{328}A$ mutant compared to His-rAp-B (data not shown; Table 1).

3.1.2. Mutations in the $G_{298}XMEN$ motif

Substitution of G_{298} by Leu, Val, Phe, Thr or Ala, M_{300} by Thr, Arg, Asp and Leu, E_{301} by Gly, Asp or Pro, and replacement of N_{302} by Leu, Lys, Tyr or Phe abolished the enzyme activity in our experimental conditions (Table 1). These results show that conservation of these residues within the GXMEN motif is necessary for the rAp-B activity.

A detailed attention was given to the G_{298} mutants obtained by site-specific saturation mutagenesis. As shown in Table 1, substitution of G_{298} by either bulky hydrophobic amino acids such as Leu and Val or an aromatic residue such as Phe completely abolished the peptidase activity. The $G_{298}A$ mutant (motif AGMEN versus GGMEN in rAp-B) exhibited no activity. Note that the sequence of this motif is GAMEN in more than 80% of the M1 family members, but GGMEN in Ap-Bs and LTA_4Hs, and AAMEN in the Thyrotropin-Releasing

Hormone degrading enzyme (TRH-DE). The presence of the methyl group of alanine in this position might be sufficient to alter the interaction with the substrate since no activity was detected with L-aa-β-NA representing the 20 amino acids.

The replacement of G_{298} by Ser or Thr led to interesting results. Both residues exhibit a moderately reactive hydroxyl group and are considered highly similar amino acids in most of the classical similarity matrixes such as PAM and BLOSUM, or Venn diagrams (http://prowl.rockefeller.edu/). While G_{298}S conserved an enzymatic activity, G_{298}T was thoroughly inactive. This observation could be linked to a different local environment necessary for the enzymatic mechanism. A slight increase of the volume residue might be also considered. Interestingly, the substitution of G_{298} by Pro led to an enzyme whose activity in crude protein extracts was higher than that of the G_{298}S mutant (90% compared to His-rAp-B; Table 1). Both mutants were expressed in Bli5 *E. coli* strain and purified. Gel electrophoresis of the final elution step of these purified proteins show only one band with a relative molecular mass around 74 kDa (data not shown). Western blotting truly identified rAp-B isoforms and demonstrated that no degradation product was present (data not shown).

3.2. Analysis of the enzymatic activity of the purified G_{298}S and G_{298}P mutants

3.2.1. Substrate specificity and catalytic properties

G_{298}S and G_{298}P mutants showed, respectively, 60% and 90% of the activity of the His-rAp-B enzyme when L-Arg-β-NA was used as substrate (Table 1). The substrate specificity of these mutants was tested using the 20 different L-amino acids β-NA. G_{298}S cleaved only L-Arg and L-Lys β-NA, whereas G_{298}P was able to hydrolyze L-Arg, L-Lys, L-Ala, L-Pro and, to a lesser extent, L-Leu β-NA (Table 2). Kinetic constants for the enzymatic reaction of both mutants and His-rAp-B protein were estimated in the substrate concentration range 1–350 μM using Lineweaver–Burk plots of 1/v against 1/[S], and Hanes–Woolf plots of [S]/v against [S] (Table 2). Substitution of G_{298} by Ser or Pro induced a decrease of k_{cat} (17.5 fold and 4.5 fold, respectively) with L-Arg β-NA. This suggested that Gly_{298} is implicated in the stabilization of the transition state during the catalysis. The effect on K_M values was less pronounced since it varies between 1.1 (G_{298}S) and 2.5 (G_{298}P) fold. With L-Lys β-NA, only the G_{298}S mutation led to an important decrease of k_{cat} (10 fold) and K_M (2.5 fold). L-Pro and L-Ala β-NA could be considered as good substrates for G_{298}P, in contrast to L-Leu β-NA. Unlike Proline, hydroxyproline-β-NA was resistant to hydrolysis by these enzymes.

3.2.2. Influence of NaCl

Addition of 0.2 M NaCl to either the purified rat testis Ap-B [3] or the recombinant enzymes expressed in baculovirus [33] and in *E. coli* [22], results in an increase in activity. Consequently, the effect of NaCl was studied by assaying His-rAp-B, G_{298}P and G_{298}S (15 nM each) enzyme activity in the presence of NaCl ranging from 0 to 2 M in 0.1 M borate buffer pH 7.4 (Fig. 1). The addition of NaCl up to 200 mM produced a gradual increase of His-rAp-B enzymatic activity, then a strong inhibition was observed at higher concentration. In contrast, the activity of G_{298}S was only slightly increased at 200 mM NaCl (1.4 fold), whereas no effect of chloride anions was observed with the G_{298}P mutant, a slight inhibition being even observed from 10 mM of salts.

3.2.3. Sensitivity to inhibitors

The inhibitory profile of purified His-rAp-B, G_{298}S, and G_{298}P was realized using L-Arg β-NA as substrate (Table 3). As previously shown for Ap-B purified from rat testis [3], and recombinant rAp-B expressed in the baculovirus [33] and *E. coli* [22], G_{298}S and G_{298}P mutants exhibit metallopeptidase properties, being inhibited by EDTA and O-phenanthroline in the milli- and micromolar concentrations, respectively. The activity of the 3 enzymes was also sensitive to the reducing agent dithiotreitol (DTT) suggesting the role of thiol groups and/or disulfide bridge(s). However, G_{298}P was less sensitive to DTT than His-rAp-B and G_{298}S. Local differences in the 3D structure of the active site of this mutant might be responsible of this difference. Enzymatic activity was not affected by PMSF, a serine protease inhibitor. Captopril, which inhibits LTA_4H in the nanomolar range [17], was poorly effective against His-rAp-B, G_{298}S and G_{298}P even at millimolar concentrations. As expected, bestatin or arphamenine A and B, which are reported to be specific inhibitors of Ap-B, were efficient against His-rAp-B (IC_{50} around 40 nM). Surprisingly, G_{298}P was not inhibited by these compounds in the nanomolar (arphamenine A and B) or micromolar (bestatine) range. The effect of these inhibitors was also less pronounced with the G_{298}S mutant as the IC_{50} were around 450 nM and 850 nM for the arphamenine B and A, respectively. This suggests that the replacement of G_{298} by Pro has induced significant modifications in the active site of the mutant.

3.2.4. Urea treatment

Urea was used to study potential differences in the folding of recombinant Ap-Bs and mutated enzymes. His-rAp-B, Bac-rAp-B, G_{298}S or G_{298}P proteins (1 μM) were incubated with various concentrations of urea (from 0 to 9 M) and their remaining activity in presence and in absence of 150 mM NaCl was assessed (Fig. 2). The activity of His-rAp-B and of G_{298}S showed similar behaviours in presence of urea. That of Bac-rAp-B and of G_{298}P seem to be more stable. A complete loss of enzymatic activity was observed depending of each enzyme when urea concentration was increased from 2 to 4 M. We assume that these results are not due to the denaturing properties of urea, but to a small uncompetitive inhibitory effect of urea on the Ap-B enzymatic activity (results not shown). A small effect of NaCl was observed, which appears to

Table 2
G_{298}P, G_{298}S and His-rAp-B kinetic parameters for the hydrolysis of different L-amino acid-β-NA substrates.[a]

Enzymes	*G_{298}P*			*G_{298}S*			His-rAp-B		
Substrates	k_{cat} (s^{-1})	K_M (μM)	k_{cat}/K_M ($M^{-1}.s^{-1}$)	k_{cat} (s^{-1})	K_M (μM)	k_{cat}/K_M ($M^{-1}.s^{-1}$)	k_{cat} (s^{-1})	K_M (μM)	k_{cat}/K_M ($M^{-1}.s^{-1}$)
L-Arg-β-Na	6.3 ± 1.3	47 ± 2	130,000	1.6 ± 1.5	102 ± 20	16000	28 ± 3	115 ± 13	240,000
L-Lys-β-Na	9.3 ± 1.4	116 ± 5	80,000	0.8 ± 0.3	485 ± 30	1600	8.8 ± 0.8	188 ± 15	47,000
L-Ala-β-Na	7.9 ± 1.7	388 ± 40	20,000	nc	nc	nc	nc	nc	nc
L-Pro-β-Na	13.4 ± 1	558 ± 22	24,000	nc	nc	nc	nc	nc	nc
L-Leu-β-Na	3 ± 1	522 ± 17	5700	nc	nc	nc	nc	nc	nc
Trans-4-hydroxy-L-Pro β-Na	nc	nc	nc	nc	nc	nc	nc	nc	nc

[a] The specificity of the enzymes was tested using the 20 different L-amino acid β-NA substrates. Substrates that were hydrolyzed by the wild-type or mutant Ap-B were used for further kinetic analyses. K_M and k_{cat} values are the means ± standard error of three independent series of tests in which each point was performed in triplicate (nc, not cleaved).

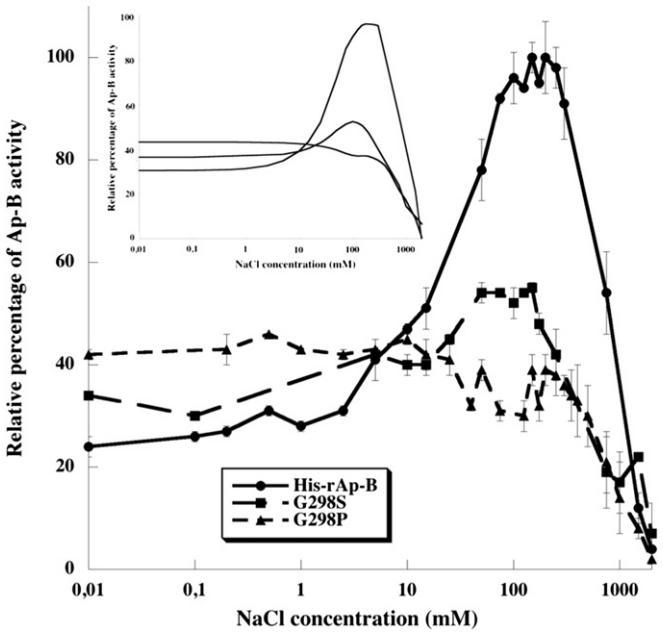

Fig. 1. Effect of NaCl concentration on His-rAp-B, $G_{298}S$ and $G_{298}P$ enzymatic activity. Activity was measured using the standard assay method described in Materials and Methods with NaCl concentrations ranging from 0 to 2 M (0, 2, 4, 6, 8, 10, 15, 20, 25, 50, 100, 150, 200, 250, 300, 350, 400, 450, 500, 750, 1000, 1500, 2000 mM NaCl, respectively). *X*-axis is represented in logarithmic scale. Activities are expressed relative to the maximum activity (100%) of the His-rAp-B enzyme obtained in presence of 200 mM NaCl. Each value is the average of at least three independent series of tests in which each point was performed in triplicate. Vertical bars represent the standard deviation between the different experiments. To simplify the reading, the same figure was added in the graph after smoothing curves.

increase the inhibitory effect of urea according to a mechanism that remains to be elucidated.

3.2.5. Activity depending of the temperature

rAp-B seems very stable to temperature. Activities from purified His-rAp-B, Bac-rAp-B, $G_{298}S$ and $G_{298}P$ proteins remain stable up to 45 °C, then strongly decreased at 55 °C and disappeared at 60 °C (Fig. 3). No obvious difference in behaviour between the different proteins was observable.

3.3. Circular dichroism analyses

The overall structures of His-rAp-B and mutants were examined using circular dichroism between 185 and 260 nm at 25 °C in 50 mM borate pH 7.4 using 3 to 7 different protein preparations (see Materials and methods section). Purified Bac-rAp-B was used as a control to ensure that there is no important difference of 3D structure between the recombinant proteins, depending of the host of expression. While the spectra of His-rAp-B and Bac-rAp-B overlapped, those of $G_{298}S$ and $G_{298}P$ mutants slightly differed (data not shown). The percentages of α helix, β structures and random coil obtained with the different samples of each different protein were accumulated and averaged (Table 4). No notable difference was observed between His-rAp-B, Bac-rAp-B and $G_{298}P$ mutant. $G_{298}S$ presents a percentage of α helix that is more pronounced at the expense of the β sheet structures. This suggests that only small structural differences may occur between wild-type and mutated enzymes.

3.4. Fluorescence spectroscopy analyses

As $G_{298}P$ exhibits original enzymatic properties, fluorescence spectra of His-rAp-B, Bac-rAp-B, $G_{298}S$ and $G_{298}P$ were performed

Table 3
Effect of inhibitors on His-rAp-B, $G_{298}P$ and $G_{298}S$ activities.[a]

Inhibitors	Concentration	His-rAp-B % of inhibition	$G_{298}P$ % of inhibition	$G_{298}S$ % of inhibition
O-phenanthroline	500 μM	81	90	84
	250 μM	67	80	75
	100 μM	6	40	40
	50 μM	0	0	10
	25 μM	0	0	0
EDTA	10 mM	71	68	78
	5 mM	65	65	75
	1 mM	53	62	69
DTT	500 μM	100	40	93
	100 μM	6	11	0
NEM	1 mM	71	69	62
PMSF	500 μM	5	6	4
Captopril	2 mM	4	8	nd
	100 μM	0	0	nd
Arphamenine A	10 μM	100	32	100
	5 μM	88	0	84
	1 μM	90	0	54
	500 nM	97	0	40
	200 nM	93	0	17
	100 nM	87	0	11
Arphamenine B	10 μM	100	30	100
	5 μM	98	10	93
	1 μM	100	1	68
	500 nM	97	0	57
	200 nM	93	0	33
	100 nM	87	0	18
Bestatine	100 μM	100	8	97
	50 μM	98	12	100
	1 μM	94	2	40

[a] The percentage of inhibition was calculated by taking as reference the amount of substrate conversion by each enzyme in absence of inhibitor (see Materials and methods section). Values are the average of three independent series of tests in which each point was performed in triplicate (nd, not determined).

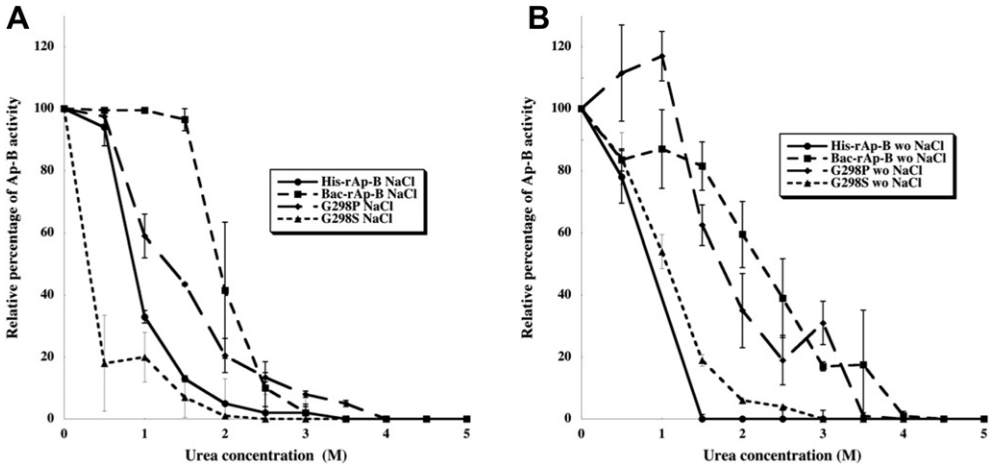

Fig. 2. Effect of urea on His-rAp-B, $G_{298}S$, $G_{298}P$ and Bac-rAp-B enzymatic activity. Activity was measured using the assay method described in Materials and Methods with urea concentrations ranging from 0 to 9 M. A loss of enzymatic activity was observed for each enzyme when urea concentration was increase to 4 M. Consequently, values obtained with urea concentrations from 5.5 to 9 M are not represented. Plotted values correspond to the following urea concentrations: 0, 0.5, 1, 1.5, 2, 2.5, 3, 3.5, 4, 4.5 and 5 M, respectively. (A) Ap-B activity in presence of 150 mM NaCl. (B) Ap-B activity in absence of NaCl. Activities are expressed relative to the maximum activity (100%) of each enzyme obtained in absence of urea. Each value is the average of at least three independent series of tests in which each point was performed in triplicate. A vertical bar represents the standard deviation between the different experiments.

to assess potential differences in the microenvironment of tryptophan residues (13 residues). Free tryptophan was used as control. The maximum of fluorescence of tryptophan was at 355 nm in aqueous buffer, whereas His-rAp-B, Bac-rAp-B, $G_{298}P$ and $G_{298}S$ showed a blue shift of about 15 nm, suggesting that these residues are probably masked to the aqueous solvent. No significant differences were observed between the spectra of the different recombinant enzymes (data not shown).

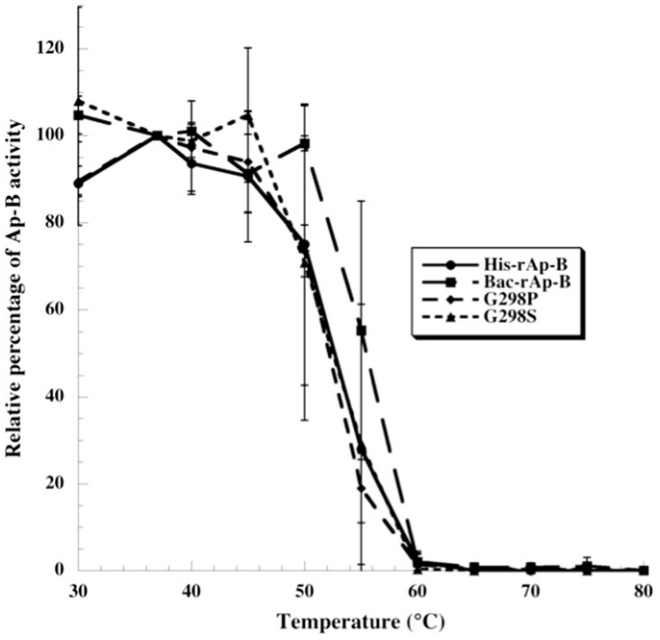

Fig. 3. Effect of the temperature on rAp-B activity. Purified His-rAp-B, $G_{298}S$, $G_{298}P$ and Bac-rAp-B proteins were preincubated at different temperatures (30, 37, 40, 45, 50, 55, 60, 65, 70, 75 and 80 °C) during 10 min, and activity was measured using the assay method described in Materials and Methods. Activities are expressed relative to the maximum activity at 37 °C (100%) of each enzyme. Each value is the average of at least three independent series of tests in which each point was performed in triplicate. A vertical bar represents the standard deviation between the different experiments.

3.5. Molecular modelling and dynamic

The 3D molecular model of rAp-B [22] was used to build the 3D structure of $G_{298}S$ and $G_{298}P$. Then, molecular dynamic simulations were performed to investigate the role that residue G_{298} plays in the catalytic mechanism of Ap-B. Simulations were carried out during 5 ns. Distances between residues of the active site and the Zn^{2+} cation or the residue in position 298 (Gly, Ser, or Pro) were analyzed. As shown in Fig. 4, the distance between S_{298} and Zn^{2+} (Fig. 4-A, -B), H_{325} (Fig. 4-D), and K_{600} (Fig. 4-F) are different compared to rAp-B and $G_{298}P$ for which the fluctuation of the distance are very similar (Fig. 4-A to -F). Distances between the mutated residue G_{298} and the G_{299} residue (the second glycine residue of the GGMEN motif) are shown as a control (Fig. 4-C). Distances between the Zn^{2+} cation and H_{325} (one of the Zn^{2+} ligands) were similar in the three molecular models (Fig. 4-E). Although the distances were not examined between all atoms, these results are confirmed regarding to distances between Zn^{2+} and several other residues: similar fluctuations were observed with P_{296}, A_{320} and D_{321} residues; differences are obtained with F_{295}, F_{297}, T_{306}, F_{307}, V_{308}, P_{310}, C_{311}, G_{599} and Q_{601} residues (data not shown). The same goes for distances between G_{298} and several residues: similar fluctuations are observed with P_{296}, T_{306}, V_{308}, P_{310}, C_{311}, A_{320} and G_{599} residues; differences are shown with F_{307}, Q_{601} (data not shown) and K_{600} (see below) residues. These results lead to the hypothesis that single mutations of amino acid residues, particularly the G_{298} in Ap-B structure could lead to local structural rearrangements explaining changes in specificity and catalytic properties.

Table 4
Secondary structure contents of recombinant Ap-B, $G_{298}S$ and $G_{298}P$ mutants.[a]

Protein	% Alpha	% Beta	% Beta turn	% Random coil
Bac-rAp-B	26 ± 7.2	24 ± 6.5	17 ± 0.3	33 ± 3.4
*His-r*Ap-B	24 ± 2	26 ± 3.2	18 ± 0.3	32 ± 1.8
$G_{298}S$	33 ± 5.3	18 ± 4.3	17 ± 0.5	32 ± 1.2
$G_{298}P$	22 ± 4	28 ± 4.1	17 ± 0.5	33 ± 1.3

[a] Percentages of alpha helix, beta sheet, beta turn and random coil from recombinant His-rAp-B, $G_{298}S$, $G_{298}P$ and Bac-rAp-B are indicated. The standard deviation between the different experiments is mentioned.

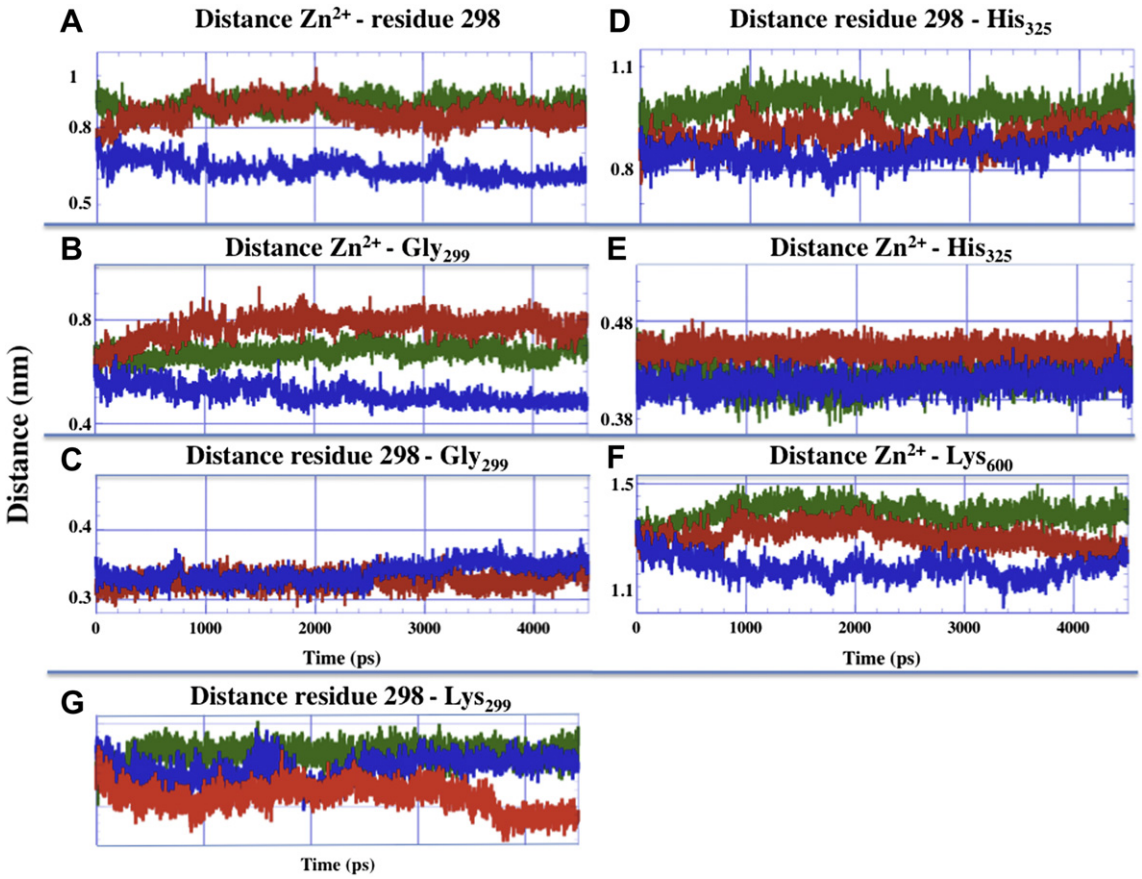

Fig. 4. Distances as a function of time between centre of masses of Zn^{2+} cation or residues and different residues in rAp-B (green), $G_{298}P$ (red) and $G_{298}S$ (blue) structural models: (A) between Zn^{2+} and G_{298} residue; (B) between Zn^{2+} and G_{299} residue; (C) between G_{299} and G_{298} residues; (D) between H_{325} and G_{298} residues; (E) between Zn^{2+} and H_{325} residue; (F) between Zn^{2+} and K_{600} residue; (G) between G_{298} and K_{600} residues (For interpretation of the references to color in this figure legend, the reader is referred to the web version of this article.).

A detailed investigation of at least 23 conformers showed that distances between the Zn^{2+} ion and its ligands are adequate and close to 2 Å in the three 3D models. However, differences in the orientation of E_{348} were observed (Fig. 5). Only one oxygen atom of E_{348} showed a good distance to form a bond with Zn^{2+} (2 Å; the second O_2 atom is at more than 4 Å) in 20 conformers of rAp-B out of 23 and 30 conformers of $G_{298}S$ out of 31. In $G_{298}P$, both oxygen atoms of E_{348} are at 2 Å of the Zn^{2+} cation (28 structural conformations out of 31) and might form bonds (Fig. 5). Thus, despite structural differences that affect their active centre and may explain their unique enzymatic activities, rAp-B and $G_{298}S$ show similar characteristics with a monodentate E_{348} ligand. Inversely, $G_{298}P$ exhibits a bidentate E_{348} ligand that could partially explain differences in catalytic mechanism (Fig. 5).

Interesting results were observed regarding the distance between P_{298} and K_{600}. After 3.5 ns of dynamic simulation (a time that might correspond to an equilibrated system), a change occurred in the distances between the Cα of both residues (Fig. 4-G). This structural modification might play an important role in the substrate (and inhibitor) specificity of the enzyme.

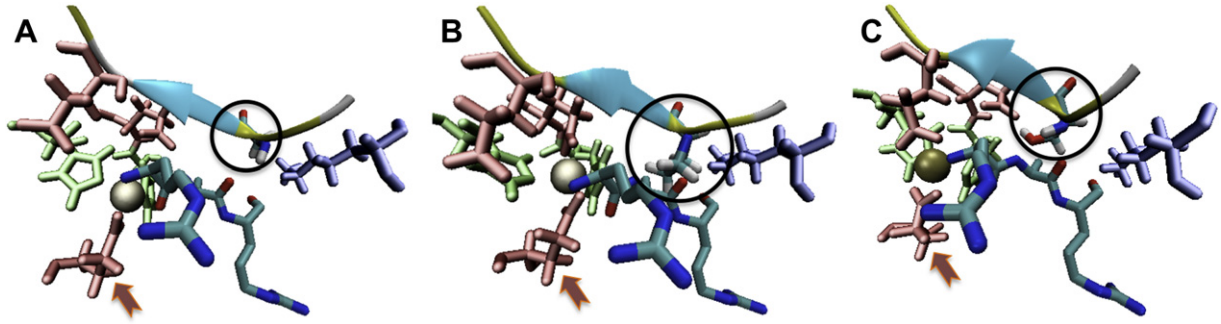

Fig. 5. Schematic representation of the active site of wild-type rAp-B, $G_{298}S$ and $G_{298}P$ proteins. The Zn^{2+} cation (sphere) and its three ligands H_{325}, H_{329} (in green) and E_{348} (in red and indicated by an arrow) are represented. The glutamate residues of the HEXXH and GXMEN motifs, E_{301} and E_{326} are also specified (in red). K_{600} residue is also indicated (in blue). G_{298} (A), P_{298} (B) and S_{298} (C) are surrounded by a circle. An Arg–Ala–Arg (RAR; light blue) tripeptide has been docked in the Ap-B active site using the DaliLite software of the Thornton group at the EMBL-EBI (For interpretation of the references to color in this figure legend, the reader is referred to the web version of this article.).

Ap-B	GGMENX^{22}HEISHX^{18}E
RNPEP-like 1	GGMENX^{22}HEISHX^{18}E
LTA$_4$H	GGMENX^{22}HEISHX^{18}E
Ap-O	**L**GM**AS**X^{23}HEI**A**HX^{20}E
Ap-N	G**A**MENX^{31}HE**LA**HX^{18}E
ERAP1	G**A**MENX^{31}HE**LA**HX^{18}E
PSA	G**A**MENX^{31}HE**LA**HX^{18}E
Ap-Q	**HA**MENX^{31}HEI**G**HX^{18}E
IRAP	G**A**MENX^{31}HE**LA**HX^{18}E
TRH-DE	**AA**MENX^{31}HEI**C**HX^{18}E
ERAP2	G**A**MENX^{31}HE**LA**HX^{18}E
Ap-A	G**A**MENX^{31}HE**LV**HX^{18}E

Fig. 6. Alignment of the consensus GXMEN and Zn^{2+} binding HEXXHX^{18}E motives of human Ap-B and other human aminopeptidases of the M1 family. The residues that are different from those from Ap-B primary structure are specified in bold and underlined. Ap-B (Uniprot KB/Swiss-prot accession number, Q9H4A4); RNPEP-like 1 (A6NKB8); LTA$_4$H (P09960); Ap-O, aminopeptidase O (Q8N6M6); Ap-N, aminopeptidase N (P15144); ERAP1 (Q9NZ08), ERAP2 (Q6P179), endoplasmic reticulum aminopeptidase 1 and 2; PSA, puromycine sensitive aminopeptidase (P55786); Ap-Q (Q6Q4G3); IRAP, insulin regulated aminopeptidase (Q9UIQ6); TRH-DE (Q9UKU6); Ap-A, glutamyl aminopeptidase (Q07075).

4. Discussion

In this study, we used site-directed mutagenesis, structural and biochemical analyses, molecular modelling and dynamics to investigate the role that residues of the GXMEN motif play in the catalytic mechanism and substrate specificity of the Ap-B glucagon- and CCK9-processing enzyme, a member of the M1 family. Nineteen mutants of the Ap-B's $G_{298}XM_{300}E_{301}N_{302}$ motif were constructed and expressed in *E. coli.* Results show that integrity of the GXMEN motif is essential for the canonical catalytic mechanism of Ap-B since mutation of these residues, except $G_{298}P$ and $G_{298}S$, abolished the activity.

4.1. The consensus motif GXMENX$^{(22\ or\ 31)}$HEXXHX^{18}E

The canonical GXMENX$^{(22\ or\ 31)}$HEXXHX^{18}E motif of the M1 family is conserved in most of the primary structures of the human aminopeptidases, except in aminopeptidase O (Ap-O; Fig. 6). For this member, 3 out of 8 residues differ [40]. Surprisingly, Ap-O exhibits a significant similarity with LTA$_4$H and Ap-B, and exhibits specificity for Arg and Asn residues *in vitro.* In Ap-B, RNPEP-like 1 and LTA$_4$H proteins, the signature is GGMENX^{22}HEISHX^{18}E (except bovine Ap-B [26]) whereas it is GAMENX^{31}HEL(A/V)HX^{18}E for aminopeptidase N (Ap-N), endoplasmic reticulum aminopeptidase 1 and 2 (ERAP1, ERAP2), insulin regulated membrane aminopeptidase (IRAP), puromycin sensitive aminopeptidase (PSA), and glutamyl aminopeptidase (Ap-A). Aminopeptidase Q (Ap-Q; HAMENX^{31}HEIGHX^{18}E) and TRH-DE (AAMENX^{31}HEICHX^{18}E) exhibit motives that could partially explain their peculiar specificity as they can cleave, respectively, a pyroglutamyl amino acid or an N-terminal amino acid residue adjacent to a proline in a peptide such as kallidin 10 [41].

4.2. Role of the GXMEN motif

For LTA$_4$H, it has been demonstrated that a tripeptide substrate, such as RAR, binds as an extended β strand antiparallel to the β strand defined by the GXM residues of the G_{268}XMEN motif [25]. The molecular model of Ap-B shows that the GXMEN motif is localized in a β hairpin facing the Zn^{2+} cation, supporting its implication in substrate binding and in the catalytic reaction (Fig. 7). The first three residues of the GAMEN motif constitutes a β strand whereas the next glutamate residue is present in a loop which could confer some flexibility in the orientation of this amino acid side chain. It seems therefore that this motif, together with the glutamate residue is essential in the positioning of the substrate and also in the binding of the transition state.

The crystal structure of LTA$_4$H with either the tripeptide RAR or RSR confirmed that E_{271}, in the GXMEN motif, interacts with the α-amino group of the bound substrate in association with E_{318} and the Zn^{2+} cation [25]. This residue is also an obvious candidate for the deprotonation of the NH^{3+} α-amino group of the substrate. That is probably why a glutamine residue is not accepted at this position for LTA$_4$H, Ap-A, Ap-N, TRH-DE and IRAP enzymes [27,28,30,31,42]. However, for TRH-DE, the function of this residue seems to be more complex since this enzyme removes specifically a pyroglutamyl residue from TRH, which does not have a free α amino group [42].

The Met residue might be implicated in the recognition of substrates, and site-directed mutagenesis studies suggested that Asn is implicated in the stabilization of the transition state [29,32,43]. The Gly residue is important for the binding of peptide

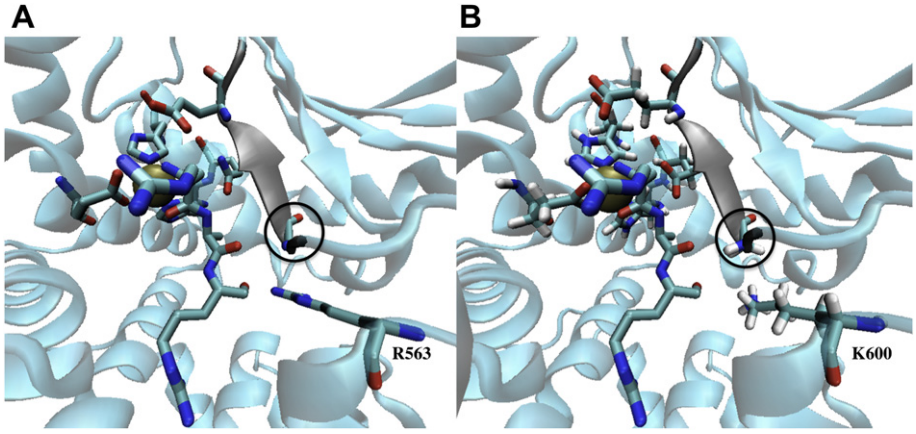

Fig. 7. Schematic representation of the active site of LTA$_4$H and rAp-B. (A) The LTA$_4$H mutated protein $E_{296}Q$ was co-crystallised with an Arg-Ala-Arg (RAR) tripeptide [25]. The residues G_{268} (surrounded by a circle), E_{271}, H_{295}, E_{296}, H_{299} and E_{318} of the consensus motif GXMENX^{22}HEXXHX^{18}E, and R_{563} implicated in an electrostatic interaction with the C-terminus of the peptide are shown. The peptide is antiparallel to and interacts with the GGMEN β-sheet (in grey). (B) The corresponding image of rAp-B structure with a RAR tripeptide substrate in its active site was obtained with the DaliLite software of the Thornton group at the EMBL-EBI. The corresponding G_{298} (surrounded by a circle), E_{301}, H_{325}, E_{326}, H_{329}, E_{348} and K_{600} amino acids of the Ap-B are indicated.

substrates since its replacement with bigger or polar residues abolishes the activity [32]. Analysis of the interaction of the peptide substrate RAR in the binding pocket of the LTA_4H shows that G_{268} and G_{269} are implicated in hydrogen bond interactions. The carbonyl oxygen of the scissile peptide bond interacts with the Zn^{2+} cation and the hydroxyl group of Y_{383} (Y_{414} for Ap-B), while the amide nitrogen interacts with the backbone carbonyl of G_{268} and G_{269} (G_{298} and G_{299} for Ap-B) present in the GGMEN motif. The carbonyl carbone is then susceptible to be attacked by a nucleophile water molecule, which is activated by E_{296} (E_{326} for Ap-B).

4.3. GXMEN motif and Ap-B

We showed here that the replacement of G_{298} by Ala, Leu, Val, Phe or Thr abolished the enzyme activity. Apolar residues such as Ala, Leu, Val or Phe are not accepted by the catalytic mechanism of Ap-B. Indeed, Leu, Val or Phe could create a steric hindrance. Although Thr has a hydroxyl group, it possesses also a hydrophobic methyl group, which could interfere with the catalytic mechanism depending on its orientation in the pocket. Replacement of G_{298} by a small and polar residue such as Ser does not affect the activity and the substrate specificity of the enzyme, but new characteristics appear, notably, a drastic decrease of the effect of chloride anions together with a lesser sensitivity to aminopeptidase inhibitors such as bestatin or arphamenine. The $G_{298}P$ mutant also revealed new catalytic properties, being able to cleave L-Arg, L-Lys, L-Ala and L-Pro β-NA. Moreover, this mutant was not sensitive to the specific inhibitors of Ap-B. This suggests that $G_{298}P$ mutation has induced key local modifications within the active site of the enzyme. A characteristic of proline residue compared to serine is that it possesses no functional groups, thus preventing participation in hydrogen bonds or in the resonance stabilization of the peptide bond. This could partly explain the different properties of mutants $G_{298}P$ and $G_{298}S$. In addition, hydroxyproline-β-NA is resistant to hydrolysis by this mutant, suggesting that this substrate could not be adapted in the same hydrophobic environment during catalysis [44]. These results show that this interaction is more crucial for the binding of the transition state since the effects are more pronounced on the k_{cat} than the K_M.

4.4. Ap-B activity and chloride anions

Enzymatic activity of many enzymes is regulated by chloride anions. The testis Angiotensine Converting Enzyme (tACE; Zn^{2+}-dipeptidyl carboxypeptidase; [45]) exhibits two Cl^--binding sites. Despite many crystallographic structures, mechanism of Cl^- activation of ACE remains unclear. A comparison of Cl^--dependent and Cl^--independent α-amylases showed that both type of enzymes can be differentiated by the presence of a loop involved in substrate binding in the case of the Cl^--dependent enzymes (as seen for members of the M1 family). The presence or absence of chloride anions in the active site is able to change the orientation of the catalytic glutamate residue implicated in the nucleophilic attack of α-glycosidic bond. All these data demonstrate that Cl^- activation is related to enzyme specificity and catalytic mechanism. Chloride anions are able to reorganize the hydrogen bond network in the active site and, therefore, to induce reorientation of the catalytic residues [46–48]. Thus, the presence of Cl^- can modulate the enzyme activity as well as its optimal pH. This phenomenon is observed with Ap-B in presence of 0.15–0.2 M NaCl and the enzyme is active in a large pH range. The LTA_4H peptidase activity is also stimulated by the presence of chloride anions (250–300 mM; [49]). As the regulatory effect of these anions follows saturation kinetics, the presence of a Cl^- binding site in the enzyme structure was proposed [49]. In contrast, no effect of Cl^- anions was observed on the LTA_4H epoxyde hydrolase activity. Because of the difference in extracellular (about 150 mM) and intracellular (3 mM) chloride concentration, it was postulated that the LTA_4H might exert a proteolytic function outside the cell [49]. The phylogenetic relationships between LTA_4H and Ap-B could lead to the hypothesis of the existence of one, or more binding sites for Cl^- anions, at, or near the active site of the Ap-B. Based on the analysis of the 3D models of $G_{298}P$ and $G_{298}S$ mutants, the replacement of a glycine residue by a larger amino acid (Pro or Ser; [Fig. 5]) could prevent the binding of chloride anions or interactions between anions and the substrates, and explain this loss of stimulation. Further studies, in particular 3D structures, are necessary to elucidate this complex mechanism.

4.5. Ap-B activity and inhibitors

In contrast to Ap-B, $G_{298}P$ and in lesser extent $G_{298}S$ are not inhibited by arphamenine A and B in the subnanomolar range. This was unexpected because $G_{298}P$ hydrolyses L-Arg and L-Lys β-NA that are structurally similar to these inhibitors (analogues of Arg-Phe and Arg-Tyr dipeptides, respectively). In addition, these mutants were less affected by bestatin, a general metalloprotease inhibitor, which is an analogue of D-Phe-Leu dipeptide.

As shown in the crystal structure of LTA_4H co-crystallised with bestatin, the Zn^{2+} cation is linked to the OH group of the Phe Cβ of bestatin and to the carbonyl group of the peptidic bond, leading to inhibition of the cleavage. Moreover, the C-terminus of bestatin, as well as the C-terminus of the RAR substrate (Fig. 7), establishes electrostatic interactions with the R_{563} and K_{565} residues of LTA_4H [23,25]. In arphamenine compounds, the NH group of the peptide bond is substituted by a methyl group and, as in bestatin, the carbon just upstream the peptide bond carries a carboxylic group. In mutated Ap-B, one or both of these differences might explain the absence of efficiency of the inhibitor that becomes unable to bind to the active site. Notably, $G_{298}S$ could establish hydrogen interactions with the peptide. Finally, Ap-B K_{600} and K_{602} residues might interact with the COO^- terminus of the substrate (as R_{563} and K_{565} with the C-terminus of bestatin in LTA_4H [23]). The presence of P_{298} or S_{298} might create sterical hindrance, which could disturb the interaction with arphamenine or bestatine and notably perturbs the electrostatic interaction, which maintains the C-terminus of the peptide substrate.

4.6. Ap-B activity, temperature and urea

We used temperature and urea to highlight some structural differences between wild-type Ap-B and G_{298} mutants. On one hand, results show that Ap-B is structurally resistant to temperature variations, at least until 50 °C. This stability might be explained by the high content of proline residues (7.5%) in Ap-B primary structure [50]. On the other hand, we also show that urea cannot be used as a denaturant agent of the Ap-B protein because it inhibits its activity at low concentration. This inhibition is probably due to the fact that urea exhibits a chemical group, similar to the guanidium group of arginine, that prevents the enzymatic cleavage.

5. Conclusions

The $G_{298}S$ and especially the $G_{298}P$ mutations cause only small local structural changes, but they are important in the catalytic mechanism of the enzyme. The substrate specificity of Ap-B is linked to the presence of a linear aliphatic chain C_3–NH (Arg) or C_4 (Lys) and a guanidium or amine function. This is in agreement with the data deduced from both the X-ray structure of LTA_4H and our model. It has been shown that D_{405} (D_{375} for LTA_4H) is implicated in an interaction with the basic amine of the P1 side chain of the

substrate [51]. Moreover, the binding pocket is hydrophobic and narrow in order to fit the aliphatic chain. This might also explain why LTA_4H and Ap-B share common characteristics. LTA_4H catalyzes LTA_4 in LTB_4 and is also able to process basic amino acids presenting an aliphatic side chain. In contrast with Ap-B, the aminopeptidase specificity of the LTA_4H is larger, able to cleave substrates such as Arg, Lys, Ala, Leu and Pro [52,53] suggesting local reorientation and/or specific amino acid interactions in the S1 pocket allowing these cleavages. Results concerning the substrate specificity of $G_{298}P$ indicate that local rearrangements induced in the β-sheet of the GXMEN motif could reorganize the active site and lead to a favourable position of hydrophobic residues such as Ala, Leu or Pro. The side chain of Proline residue is bonded both to the amino group and to the α-carbon leading to a cyclic structure. This cyclic structure induces important constraints on the conformation of the polypeptide backbone. The bond most likely affected in $G_{298}P$ is the Phe_{297}–CO–NH–Pro_{298} bond. The mutation could induce a different orientation of the side chain of the Phe residue and a steric hindrance in the S1 pocket implicated in the binding of the P1 residue of the substrate. As there is no difference in the GXMEN motif of Ap-B and LTA_4H, their differences in substrate specificity do not only depend on this motif. Contrary to the other members of the M1 family, Ap-B and LTA_4H exhibit a peculiar GGMEN motif with two Gly residues implicated in hydrogen bonds with the peptidic bond of the substrate. Interestingly, a Tyr residue is present in LTA_4H just upstream this GGMEN signature, while it is a Phe residue in Ap-B. Therefore, it will be interesting to mutate this amino acid into a Tyr residue to verify if there is some difference in the specificity of Ap-B activity. Indeed, recent studies have shown that the corresponding Ala residue in IRAP primary structure is implicated in substrate and inhibitor specificity [54]. All these observations will provide some insights into the different substrate specificity of the M1 family aminopeptidases. Further experiments are necessary to encompass the complex role of this GXMEN motif in the catalytic mechanism of the proteolysis of physiological substrates by Ap-B and other M1 family members.

Acknowledgments

This work was supported by funds from the University Pierre et Marie Curie (UPMC, ER3), the University Denis Diderot (UMR S 665), the Institut National de la Santé et de la Recherche Médicale (INSERM, UMR S 665) and the Institut National de Transfusion sanguine (INTS, UMR S 665).

We thank Drs S. Fermandjian, L. Zargarian (UMR 8113 CNRS, Villejuif France) and C. El Amri (UR4 UPMC, Paris, France) for their help in circular dichroism and helpful discussions, and Drs D. Deville-Bonne and D. Topalis (ER3 UPMC, Paris, France) for their help in fluorescence spectroscopy.

References

[1] V. Chesneau, A.R. Pierotti, N. Barré, C. Créminon, C. Tougard, P. Cohen, Isolation and characterization of a dibasic selective metalloendopeptidase from rat testis that cleaves at the aminoterminus of arginine residues, J. Biol. Chem. 269 (1994) 2056–2061.
[2] A.V. Azaryan, V.Y.H. Hook, Unique cleavage specificity of "prohormone thiol protease" related to proenkephalin processing, FEBS Lett. 341 (1994) 197–202.
[3] S. Cadel, A.R. Pierotti, T. Foulon, C. Creminon, N. Barré, D. Segretain, P. Cohen, Aminopeptidase-B in the rat testis: isolation, functional properties and cellular localization in the seminiferous tubules, Mol. Cell. Endocrinol. 110 (1995) 149–160.
[4] T. Foulon, S. Cadel, A. Prat, V. Chesneau, V. Hospital, D. Segretain, C. Tougard, P. Cohen, NRD convertase and Aminopeptidase B: two putative processing metallopeptidases with a selectivity for basic residues, Ann. Endocrinol. 58 (1997) 357–364.
[5] S. Cadel, C. Piesse, C. Gouzy-Darmon, P. Cohen, T. Foulon, Aminopeptidase B: from protein to gene, Curr. Top. Pept. Prot. Res. 6 (2004) 37–45.
[6] G. Fontes, A.D. Lajoix, F. Bergeron, S. Cadel, A. Prat, T. Foulon, R. Gross, S. Dalle, D. Le-Nguyen, F. Tribillac, D. Bataille, Miniglucagon-generating endopeptidase, which processes glucagon into miniglucagon, is composed of NRD convertase and aminopeptidase B, Endocrinology 146 (2005) 702–712.
[7] D. Bataille, Pro-protein convertases in intermediary metabolism: islet hormones, brain/gut hormones and integrated physiology, J. Mol. Med. 85 (2007) 673–684.
[8] V. Hook, S. Yasothornsrikul, D. Greenbaum, K.F. Medzihradszky, K. Troutner, T. Toneff, R. Bundey, A. Logrinova, T. Reinheckel, C. Peters, M. Bogyo, Cathepsin L and Arg/Lys aminopeptidase: a distinct prohormone processing pathway for the biosynthesis of peptide neurotransmitters and hormones, Biol. Chem. 385 (2004) 473–480.
[9] M.C. Beinfeld, L. Funkelstein, T. Foulon, S. Cadel, K. Kitagawa, T. Toneff, T. Reinheckel, C. Peters, V. Hook, Cathepsin L plays a major role in cholecystokinin production in mouse brain cortex and in pituitary AtT-20 cells: protease gene knockout and inhibitor studies, Peptides 10 (2009) 1882–1891.
[10] V. Hook, L. Funkelstein, T. Toneff, C. Mosier, S.R. Hwang, Human pituitary contains dual cathepsin L and prohormone convertase processing pathway components involved in converting POMC into the peptide hormones ACTH, alpha-MSH, and beta-endorphin, Endocrine 35 (2009) 429–437.
[11] T. Foulon, S. Cadel, V. Chesneau, M. Draoui, A. Prat, P. Cohen, Two novel metallopeptidases with a specificity for basic residues. Functional properties, structure and cellular distribution, Ann. N.Y. Acad. Sci. 780 (1996) 106–120.
[12] S. Cadel, T. Foulon, A. Viron, A. Balogh, S. Midol-Monnet, N. Noel, P. Cohen, Aminopeptidase B from the rat testis is a bifunctional enzyme structurally related to leukotriene-A_4 hydrolase, Proc. Natl. Acad. Sci. U.S.A. 94 (1997) 2963–2968.
[13] A. Balogh, S. Cadel, T. Foulon, R. Picart, A. Der Garabedian, A. Rousselet, C. Tougard, P. Cohen, Aminopeptidase B: a processing enzyme secreted and associated with the plasma membrane of rat pheochromocytoma (PC12) cells, J. Cell Sci. 111 (1998) 161–169.
[14] G. Thoidis, T. Kupriyanova, J.M. Cunningham, P. Chen, S. Cadel, T. Foulon, P. Cohen, R. Fine, K.V. Kandror, Glucose transporter Glut3 is targeted to secretory vesicles in neurons and PC12 cells, J. Biol. Chem. 274 (1999) 14062–14066.
[15] C. Piesse, M. Tymms, E. Garrafa, C. Gouzy, M. Lacasa, S. Cadel, P. Cohen, T. Foulon, Human aminopeptidase B (rnpep) on chromosome 1q32.2: complementary DNA, genomic structure and expression, Gene 292 (2002) 129–140.
[16] C. Piesse, S. Cadel, C. Gouzy-Darmon, J.C. Jeanny, V. Carrière, D. Goidin, L. Jonet, D. Gourdji, P. Cohen, T. Foulon, Expression of aminopeptidase B in the developing and adult rat retina, Exp. Eye Res. 79 (2004) 639–648.
[17] J.Z. Haeggström, F. Tholander, A. Wetterholm, Structure and catalytic mechanisms of leukotriene A4 hydrolase, Prostaglandins Other Lipid Mediat. 83 (2007) 198–202.
[18] N.D. Rawlings, A.J. Barrett, Evolutionary families of peptidases, Biochem. J. 290 (1993) 205–218.
[19] N.M. Hooper, Families of zinc metalloproteases, FEBS Lett. 354 (1994) 1–6.
[20] N.D. Rawlings, F.R. Morton, C.Y. Kok, J. Kong, A.J. Barrett, MEROPS: the peptidase database, Nucleic Acids Res. 36 (2007) D320–325.
[21] T. Foulon, S. Cadel, P. Cohen, Molecules in Focus: Aminopeptidase B (EC 3.4.11.6), Int. J. Biochem. Cell Biol. 31 (1999) 747–750.
[22] L. V-Pham, S. M-Cadel, C. Gouzy-Darmon, C. Hanquez, M.C. Beinfeld, P. Nicolas, C. Etchebest, T. Foulon, Aminopeptidase B, a glucagon-processing enzyme: site directed mutagenesis of the Zn^{2+}-binding motif and molecular modeling, BMC Biochem. 8 (2007) 21.
[23] M.M. Thunnissen, P. Nordhund, J.Z. Häeggstrom, Crystal structure of human leukotriene A_4 hydrolase, a bifunctional enzyme in inflammation, Nat. Struct. Biol. 8 (2001) 131–135.
[24] B.W. Matthews, Structural basis of the action of thermolysin and related zinc peptidases, Acc. Chem. Res. 21 (1988) 333–340.
[25] F. Tholander, A. Muroya, B.P. Roques, M.C. Fournié-Zaluski, M.M. Thunnissen, J.Z. Haeggström, Structure-based dissection of the active site chemistry of leukotriene A4 hydrolase: implications for M1 aminopeptidases and inhibitor design, Chem. Biol. 15 (2008) 920–929.
[26] R. S-Hwang, A. O'Neill, S. Bark, T. Foulon, V. Hook, Secretory vesicle aminopeptidase B related to neuropeptide processing: molecular identification and subcellular localization to enkephalin- and NPY-containing chromaffin granules, J. Neurochem. 100 (2007) 1340–1350.
[27] N. Luciani, C. Marie-Claire, E. Ruffet, A. Beaumont, B.P. Roques, M.C. Fournié-Zaluski, Characterization of Glu350 as a critical residue involved in the N-terminal amine binding site of aminopeptidase N (EC 3.4.11.2): insights into its mechanism of action, Biochemistry 37 (1998) 686–692.
[28] G. Vazeux, X. Iturrioz, P. Corvol, C. Llorens-Cortes, A glutamate residue contributes to the exopeptidase specificity in aminopeptidase A, Biochem. J. 334 (1998) 407–413.
[29] X. Iturrioz, R. Rozenfeld, A. Michaud, P. Corvol, C. Llorens-Cortes, Study of asparagine 353 in aminopeptidase A: characterization of a novel motif (GXMEN) implicated in exopeptidase specificity of monozinc aminopeptidases, Biochemistry 40 (2001) 14440–14448.
[30] P.G. Laustsen, S. Vang, T. Kristensen, Mutational analysis of the active site of human insulin-regulated aminopeptidase, Eur. J. Biochem. 268 (2001) 98–104.
[31] P.C. Rudberg, F. Tholander, M.M. Thunnissen, J.Z. Haeggstrom, Leukotriene A_4 hydrolase/aminopeptidase. Glutamate 271 is a catalytic residue with specific roles in two distinct enzyme mechanisms, J. Biol. Chem. 277 (2002) 1398–1404.

[32] S. Ye, S.Y. Chai, R.A. Lew, A.L. Albiston, Insulin-regulated aminopeptidase: analysis of peptide substrate and inhibitor binding to the catalytic domain, Biol. Chem. 388 (2007) 399–403.
[33] S. Cadel, C. Gouzy-Darmon, S. Petres, C. Piesse, M.C. Beinfeld, P. Cohen, T. Foulon, Expression and purification of rat recombinant aminopeptidase B secreted from baculovirus infected insect cells, Prot. Exp. Pur. 36 (2004) 19–30.
[34] A.A. Canutescu, A.A. Shelenkov, R.L. Dunbrack Jr., A graph theory algorithm for protein side-chain prediction, Prot. Sci. 12 (2003) 2001–2014.
[35] H. Bekker, H.J.C. Berendsen, E.J. Dijkstra, S. Achterop, R. van Drunen, D. van der Spoel, A. Sijbers, H. Keegstra, B. Reitsma, M.K.R. Renardus, Gromacs: a parallel computer for molecular dynamics simulations. in: R.A. de Groot, J. Nadrchal (Eds.), Physics Computing 92. World Scientific, Singapore, 1993.
[36] H.J.C. Berendsen, D. van der Spoel, R. van Drunen, GROMACS: A message-passing parallel molecular dynamics implementation, Comp. Phys. Commun. 91 (1995) 43–56.
[37] E. Lindahl, B. Hess, D. van der Spoel, GROMACS 3.0: a package for molecular simulation and trajectory analysis, J. Mol. Mod. 7 (2001) 306–317.
[38] D. van der Spoel, E. Lindahl, B. Hess, G. Groenhof, A.E. Mark, H.J.C. Berendsen, GROMACS: fast, flexible and free, J. Comp. Chem. 26 (2005) 1701–1718.
[39] C. Oostenbrink, A. Villa, A.E. Mark, W.F. Van Gunsteren, A biomolecular force field based on the free enthalpy of hydration and solvation: The GROMOS force-field parameter sets 53A5 and 53A6, J. Comp. Chem. 25 (2004) 1656–1676.
[40] A. Diaz-Perales, V. Quesada, L.M. Sanchez, A.P. Ugalde, M.F. Suarez, A. Fueyo, C. Lopez-Otin, Identification of human aminopeptidase O, a novel metalloprotease with structural similarity to aminopeptidase B and leukotriene A_4 hydrolase, J. Biol. Chem. 280 (2005) 14310–14317.
[41] M. Maruyama, A. Hattori, Y. Goto, M. Ueda, M. Maeda, H. Fujiwara, M. Tsujimoto, Laeverin/aminopeptidase Q, a novel bestatin-sensitive leucine aminopeptidase belonging to the M1 family of aminopeptidases, J. Biol. Chem. 282 (2007) 20088–20096.
[42] T. Papadopoulos, J.A. Kelly, K. Bauer, Mutational analysis of the thyrotropin-releasing hormone-degrading ectoenzyme. Similarities and differences with other members of the M1 family of aminopeptidases and thermolysin, Biochemistry 40 (2001) 9347–9355.
[43] K. Ito, Y. Nakajima, Y. Onohara, M. Takeo, K. Nakashima, F. Matsubara, T. Ito, T. Yoshimoto, Aminopeptidase N (Proteobacteria Alanyl aminopeptidase) from *Escherichia coli*: crystal structure and conformational change of the methionine 260 residue involved in substrate recognition, J. Biol. Chem. 281 (2006) 33664–33676.
[44] Y. Nakajima, K. Ito, M. Sakata, Y. Xu, K. Nakashima, F. Matsubara, S. Hatakeyama, T. Yoshimoto, Unusual extra space at the active site and high activity for acetylated hydroxyproline of prolyl aminopeptidase from serratia marcescens, J. Bacteriol. 188 (2006) 1599–1606.
[45] R. Natesh, S.L. Schwager, E.D. Sturrock, K.R. Acharya, Crystal structure of the human angiotensin-converting enzyme-lisinopril complex, Nature 421 (2003) 551–554.
[46] N. Aghajari, G. Feller, C. Gerday, R. Haser, Structural basis of alpha-amylase activation by chloride, Prot. Sci. 11 (2002) 1435–1441.
[47] R. Maurus, A. Begum, H.H. Kuo, A. Racaza, S. Numao, C. Andersen, J.W. Tams, J. Vind, C.M. Overall, S.G. Witthers, G.D. Brayer, Structural and mechanistic studies of chloride induced activation of human pancreatic α-amylase, Prot. Sci. 14 (2004) 743–755.
[48] M. Qian, H. el Ajandouz, F. Payan, V. Nahoum, Molecular basis of the effects of chloride ion on the acid-base catalyst in the mechanism of pancreatic alpha-amylase, Biochemistry 44 (2005) 3194–3201.
[49] A. Wetterholm, J.Z. Haeggström, Leukotriene A4 hydrolase: an anion activated peptidase, Biochim. Biophys. Acta 1123 (1992) 275–281.
[50] H. Fu, G.R. Grimsley, A. Razvi, J.M. Scholtz, C.N. Pace, Increasing protein stability by improving Beta-turns, Proteins 77 (2009) 491–498.
[51] K.M. Fukasawa, J. Hirose, T. Hata, Y. Ono, Aspartic acid 405 contributes to the substrate specificity of aminopeptidase B, Biochemistry 45 (2006) 11425–11431.
[52] L. Orning, G. Krivi, G. Bild, J. Gierse, S. Aykent, F.A. Fitzpatrick, Inhibition of leukotriene A4 hydrolase/aminopeptidase by captopril, J. Biol. Chem. 266 (1991) 16507–16511.
[53] F. Tholander, J.Z. Haeggström, Assay for rapid analysis of the tri-peptidase activity of LTA4 hydrolase, Proteins 67 (2007) 1113–1118.
[54] S. Ye, S.Y. Chai, R.A. Lew, D.B. Ascher, C.J. Morton, M.W. Parker, A.L. Albiston, Identification of modulating residues defining the catalytic cleft of insulin-regulated aminopeptidase, Biochem. Cell Biol. 86 (2008) 251–261.